Saudi Journal of Biological Sciences 26 (2019) 1411–1417

Contents lists available at ScienceDirect

Saudi Journal of Biological Sciences

journal homepage: www.sciencedirect.com

Original article

Phorate triggers oxidative stress and mitochondrial dysfunction to enhance micronuclei generation and DNA damage in human lymphocytes

Quaiser Saquib [a,*], Mohammad Faisal [b], Sabiha Mahmood Ansari [b], Rizwan Wahab [a]

[a] Zoology Department, College of Sciences, King Saud University, P.O. Box 2455, Riyadh 11451, Saudi Arabia
[b] Department of Botany & Microbiology, College of Sciences, King Saud University, P.O. Box 2455, Riyadh 11451, Saudi Arabia

ARTICLE INFO

Article history:
Received 12 February 2019
Revised 2 April 2019
Accepted 9 April 2019
Available online 10 April 2019

Keywords:
Phorate
DNA damage
Micronuclei
Oxidative stress
Lymphocytes
Insecticides

ABSTRACT

Herein, we studied phorate for its toxicological effects in human lymphocytes. Phorate treatment for 3 h has induced significant increase in the lymphocytic DNA damage. Compared to control, comet data from highest concentration of phorate (1000 μM) showed 8.03-fold increase in the Olive tail moment (OTM). Cytokinesis blocked micronucleus (CBMN) assay revealed 6.4-fold increase in binucleated micronucleated (BNMN) cells following the exposure with phorate (200 μM) for 24 h. The nuclear division index (NDI) in phorate (200 μM) treated cells reduced to 1.8 vis-à-vis control cells showed NDI of 1.94. Comparative to untreated control, 60.43% greater DCF fluorescence was quantitated in lymphocytes treated with phorate (500 μM), affirming reactive oxygen species (ROS) generation and oxidative stress. Flow cytometric data of phorate (200 μM) treated lymphocytes showed 81.77% decline in the fluorescence of rhodamine 123 (Rh123) dye, confirming the perturbation of mitochondrial membrane potential ($\Delta\Psi m$). Calf thymus DNA (ct-DNA) treated with phorate (1000 μM) exhibited 2.3-fold higher 8-Hydroxy-2′-deox yguanosine (8-oxodG) DNA adduct formation, signified the oxidative DNA damage. The alkaline unwinding assay revealed 4.0 and 6.5 ct-DNA strand breaks when treated to phorate and phorate-Cu (II) complex. Overall, the data unequivocally suggests the cyto- and genotoxic potential of phorate in human lymphocytes, which may induce comparable toxicological consequences in persons occupationally or non-occupationally exposed to insecticide phorate.

1. Introduction

Since many decades environmental pollution pertaining to the tremendous application of organophosphorus (OPs) insecticides have been a serious issue. The widespread involvement of OPs in several commodities led their residual appearance in food, drinking water and environment (Kashanian et al., 2008). Alone in 2014, the global consumption of active ingredients containing OPs insecticides reached to 29972.53 tonnes (Zhang, 2018). The persistent and bio-accumulative properties of pesticides classify them as an environmental contaminant and precursor of diverse human health ailments. Great concern has been made towards the cholinergic effects of OPs insecticides. The OPs insecticides preferentially bind to impair the functionality of acetylcholinesterase. Perpetual signalling of neurons triggers cell death by asphyxiation has been observed due to acetylcholinesterase inhibition (Forsyth and Chambers, 1989). OPs insecticides encompass the thiophosphoryl bond (P═S) or phosphoryl bond (P═O) moiety. Metabolites of OPs insecticides harboring these groups have been attributed as potent genotoxicants (Garrett et al., 1986; Williams et al., 2006).

Phorate is a class I extremely toxic insecticide, critically known for its anti-acetylcholinesterase activity by the accumulation of acetylcholine, which hampers the synaptic transmission in neuronal cholinergic areas (Assis et al., 2012). Phorate oxon, a metabolite of phorate has been recently found to inhibit the acetylcholinesterase activity of human, guinea pig and rat (Moyer et al., 2018). Phorate has been detected in several food commodities above than the limit values (Wauchope et al., 1992;

* Corresponding author.
E-mail address: quaiser.saquib0@gmail.com (Q. Saquib).
Peer review under responsibility of King Saud University.

Production and hosting by Elsevier

https://doi.org/10.1016/j.sjbs.2019.04.008
1319-562X/

Zambonin et al., 2004; Pagliuca et al., 2006). Workers engaged in the formulation of phorate showed inhibition of testosterone metabolism, sister chromatid exchange, chromosomal aberrations, and DNA damage (De Ferrari et al., 1991; Grover et al., 2003; Usmani et al., 2003). Phorate reported to induced cytogenetic changes, alters mitochondrial membrane functionality ($\Delta\Psi m$) and ROS generation in different test systems (Sobti et al., 1982; Grover and Malhi, 1985; Lin et al., 1987; Malhi and Grover, 1987; Dhingra et al., 1990; Saquib et al., 2011; Saquib et al., 2012b). Earlier, we have demonstrated that phorate exposed rats exhibited cyto-genotoxic anomalies and cell death via induction of caspases and *p53* genes (Saquib et al., 2012a). Nonetheless, it is hard to find any report addressing the interaction mechanism of phorate-DNA, and its genotoxic potential in human cells. Hence, we aimed to study the phorate treated human lymphocytes for (i) oxidative stress (ii) dysfunction of $\Delta\Psi m$ (iii) cytogenetic and genotoxic responses (iv) quantifying 8-oxodG adduct formation and strand breaks in DNA.

2. Materials and methods

2.1. Comet assay

DNA damage was quantitated following the previous method (Saquib et al., 2009). Lymphocytes were isolated using histopaque from the whole blood of a healthy male donor having no history of the following habits *viz.* alcohol, tobacco, medication and heavy physical activity. Lymphocytes were suspended in 1 ml of RPMI-1640 containing phorate (10, 100, 250, 500, 750, 1000 μM). The treated cells were kept in a CO_2 incubator (5%) for 3 h at 37 °C. Comet slides were prepared in low melting (0.5%) and normal melting agarose (1%). Lysis was done for overnight followed by the unwinding and electrophoresis (buffer pH > 13) of cells at 24 V (300 mA) for 30 min. All slides were then subjected to neutralization, staining of cells were done with 20 μg/ml of ethidium bromide. DNA damage was analyzed on a fluorescence microscope (Nikon Eclips 80i, Japan) equipped with software (Comet Assay IV, Perceptive Instruments, Suffolk, UK).

2.2. CBMN assay

Phorate induced CBMN formation was quantified in whole blood as explained earlier (Saquib et al., 2009). Blood (0.5 ml) were treated with phorate (50, 100 and 200 μM) for 24 h and incubated at 37 °C in CO_2 (5%) incubator. Furthermore, blood was pelleted at 1000 rpm, washed and resuspended in RPMI-1640 media without phorate. After the completion of 44 h of culture, cyto B (6 μg/ml) was added and continued for incubation till 72 h. Blood was finally pelleted by centrifugation (1000 rpm, 10 min) with subsequent treatment of cells with hypotonic solution (KCl 0.56%) and fixed with glacial acetic acid:methanol (1:3) for 24 h at 4 °C, followed by slide preparation. Staining was done separately with 6 μg/ml propiodium iodide and 6% Giemsa stain in PBS. Micronuclei counting was done from 1000 binucleated cells following the standard criteria (Bonassi et al., 2001). To determine the nuclear division index (NDI) in treated cells, 500 binucleated cells were separately counted (Saquib et al., 2009).

2.3. Quantification of intracellular ROS

Phorate induced ROS generation was quantitated using fluorescence spectroscopy following our previous method (Saquib et al., 2009). 2×10^6 lymphocytes were exposed to phorate (50, 100, 250 and 500 μM) and incubated (5% CO_2) at 37 °C for 24 h. After incubation, cells were centrifuged and pellets were resuspended in saline buffer (2 ml), followed by staining with DCFH-DA (5 μM) at 37 °C. After 1 h of staining, washing was done and pellets were resuspended in 3 ml of PBS. Fluorescence of dye was recorded on spectrofluorophotometer (Shimadzu RF5301PC, Japan) at λ_{ex} 485 and λ_{em} 525 nm.

2.4. Flow cytometric quantitation of mitochondrial membrane potential ($\Delta\Psi m$)

Effect of phorate on $\Delta\Psi m$ of lymphocytes were quantitated following our previous method (Dwivedi et al., 2012). In brief, 2×10^6 lymphocytes were treated for 24 h with 50, 100 and 200 μM of phorate and incubated in CO_2 (5%) incubator at 37 °C. Cells were centrifuged (3000 rpm, 5 min) followed by resuspension of cells in 500 μl PBS. Cells were stained for 1 h with 5 μg of Rh123 in CO_2 (5%) incubator, followed by washing with PBS. Fluorescence of 10,000 stained cells were recorded on flow cytometer at FL1-H channel with excitation wavelength of 488 nm (Epics XL/Xl-MCL, Beckman Coulter USA).

2.5. Quantitation of 8-oxodG by ELISA

Formation of 8-oxodG in ct-DNA was quantified by following the method as described previously (Dwivedi et al., 2012). ct-DNA in the concentration range of 500, 1000, 1500 and 2000 ng were taken as untreated control. Fixed concentration of phorate (1000 μM) was used to expose the ct-DNA (500, 1000, 1500 and 2000 ng) and mixtures were subjected to white light exposure for 1 h. For positive control, fixed concentration of methylene blue (1000 μM) was used for treating the ct-DNA (500, 1000, 1500 and 2000 ng). After the exposure time, all samples were oven dried in a 96 well plate at 40 °C for 24 h. Blocking of non-specific sites were done for 3 h with BSA (3%) at 37 °C. Samples were incubated with primary antibody (1:100,000) (goat anti 8-hydroxyguanosine) for 2 h. Samples were washed with TMB 1X, followed by incubation with 1:25000 dilution of donkey anti sheep/goat IgG:HRP for 2 h at 37 °C. Reaction was stopped using 2 M H_2SO_4, and absorbance was taken at 450 nm using a microplate reader (Labsystems, USA). Commercially available 8-oxodG, as a standard, was used for preparing the calibration curve.

2.6. Alkaline unwinding assay

Strand breaks in phorate treated ct-DNA was done using hydroxyapatite batch procedure (Saquib et al., 2009). ct-DNA (100 μg) was treated with phorate in the molar ratio from 1:2 to 1:10 with or without 100 μM Cu (II). All tubes were incubated for 30 min at 37 °C followed by processing of samples. Elution of ct-DNA (single stranded) from hydroxyapatite matrix was done using 20% formamide in 0.125 M potassium phosphate buffer (pH 7.0). The duplex DNA was removed by 20% formamide in 0.5 M potassium phosphate buffer (pH 7.0). DNA breaks were calculated as described earlier by Saquib et al. (2009).

3. Results

3.1. Quantitation of DNA damage

Lymphocytes showed increased DNA damage after treatment with phorate (10–1000 μM) (Fig. 1). Phorate exposure at 1000 μM showed OTM value of 26.12 ± 1.97 as compared to the OTM of untreated (3.25 ± 0.08) and DMSO (3.72 ± 0.09) controls (Table 1). The extent of DNA damage by phorate at 1000 μM was almost similar to the damage induced by positive control, ethyl methane sulfonate (EMS). Variations in DNA damage in phorate treated cells

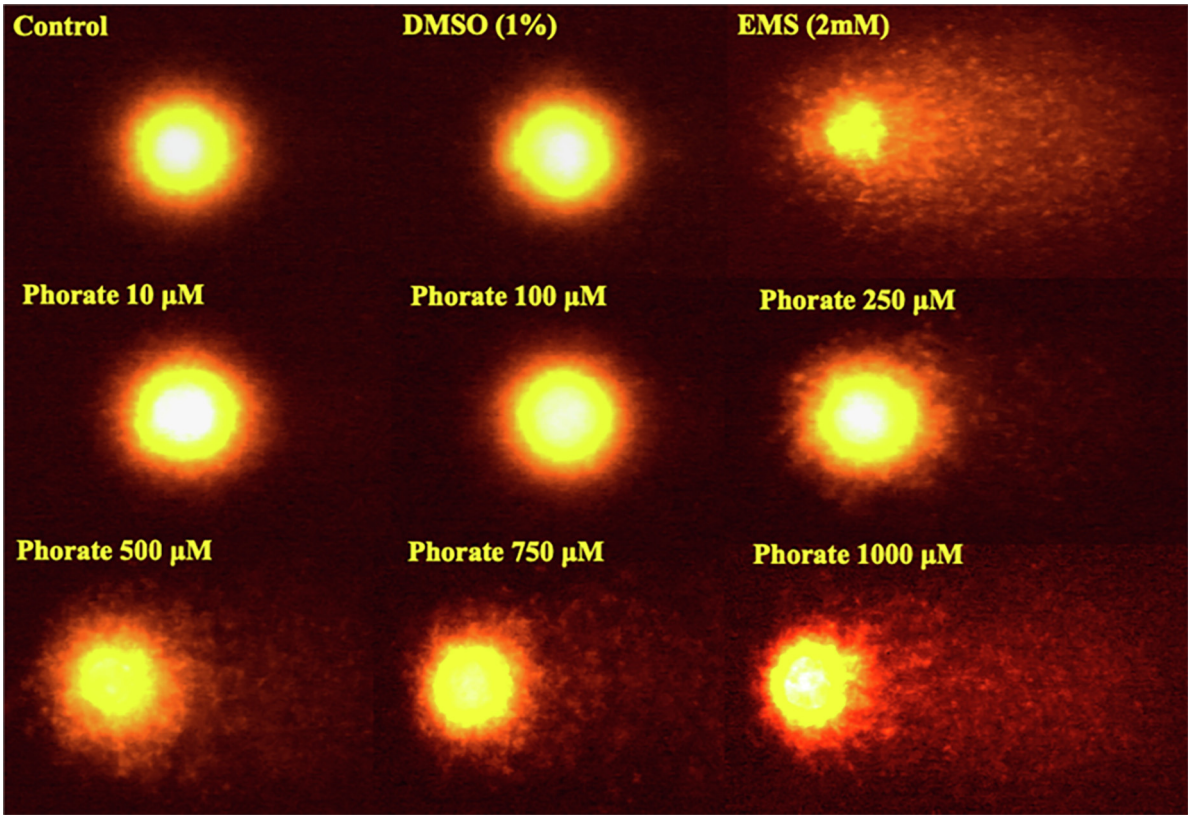

Fig. 1. Epi-fluorescence comet images of phorate showing DNA damage in human lymphocytes after 3 h of exposure.

Table 1
Phorate-induced DNA damage in human lymphocytes analyzed using different parameters of comet assay.

Groups	Olive tail moment (Arbitrary Unit)	Tail DNA (%)	Tail length (µm)
Control	3.25 ± 0.08	7.08 ± 0.17	57.61 ± 3.85
DMSO (0.5%)	3.72 ± 0.09	9.27 ± 0.30	63.03 ± 5.19
EMS (2 mM)	30.52 ± 3.48***	38.63 ± 1.95***	187.57 ± 12.70***
Phorate (µM)			
10	4.07 ± 0.16	10.03 ± 0.54	74.72 ± 9.95
100	5.89 ± 0.44	12.58 ± 0.55**	123.19 ± 16.16**
250	9.21 ± 1.43*	16.46 ± 1.00***	163.36 ± 29.93***
500	12.58 ± 2.23**	19.73 ± 2.08***	191.86 ± 11.71***
750	18.30 ± 1.99***	23.03 ± 1.05***	238.08 ± 19.66***
1000	26.12 ± 1.97***	28.13 ± 0.76***	261.84 ± 17.98***

Data represent the mean ± SEM of three experiments. *$p < 0.05$; **$p < 0.01$; ***$p < 0.001$; EMS: Ethyl methanesulfonate; DMSO: dimethysulfoxide.

were observed (Supplementary Fig. 1). At 250 µM, the values of phorate-treated cells vary from 4 to 16. At this concentration 20% of cells showed OTM of 10. While 500–1000 µM exposure showed OTM > 20, which gradually enhanced from 7 to 76%. The positive control (EMS) showed 100% cells exhibited OTM > 20, comparatively 91% of control cells were having OTM of 4.

3.2. BNMN formation in lymphocytes

An enhancement in BNMN formation was found after phorate treatment. The representative images of phorate treated lymphocytes clearly show the presence of micronucleus, while the controls showed typical binucleated cells without micronuclei (Fig. 2). Average BNMN at 50, 100 and 200 µM of phorate were found 11, 16.5 and 26.5. Comparatively, the untreated control, solvent control and positive control exhibited 4.1, 5.0 and 15.3 BNMN cells. The NDI value determined for the phorate (50, 100 and 200 µM) treated groups were 1.92, 1.89 and 1.80, relatively the untreated control showed NDI of 1.94 (Table 2).

3.3. Intracellular ROS generation by phorate

Human lymphocytes cultured with phorate for 24 h showed enhancement in the fluorescence emission spectra of DCFH-DA stained cells (Fig. 3A). Comparative to control, phorate exposed cells showed significant increase in the oxidation of DCFH-DA dye to DCF. Cells treated with phorate in the range of 50–500 µM showed 17% to 60.43% higher fluorescence intensity of DCF. H_2O_2 (400 µM) showed 19% and 1% DMSO showed 3.11% increase in DCF fluorescence (Fig. 3B).

3.4. Effect of phorate on $\Delta\psi m$

Flow cytometric analysis of phorate treated and untreated human lymphocytes exhibited distinctive variations in the fluorescence of Rh123 stained cells (Fig. 4A). Compared to the untreated control, human lymphocytes treated with phorate (50, 100 and 200 µM) for 24 h significantly perturbed the functionality of mitochondria, manifested as reduction in Rh123 fluorescence from 71.18%, 75.65% and 81.77%, respectively (Fig. 4B).

3.5. 8-oxodG formation in phorate treated ct-DNA

Exposure of ct-DNA with phorate resulted in 8-oxodG adduct formation. Compared to control, ct-DNA at the concentrations of 500, 1000, 1500 and 2000 ng treated to a fixed concentration of phorate (1000 µM) induced 1.3, 1.8, 2.1 and 2.3-fold higher 8-oxodG adduct formation. The frequency of 8-oxodG formation by phorate was higher than the positive control. Under the similar

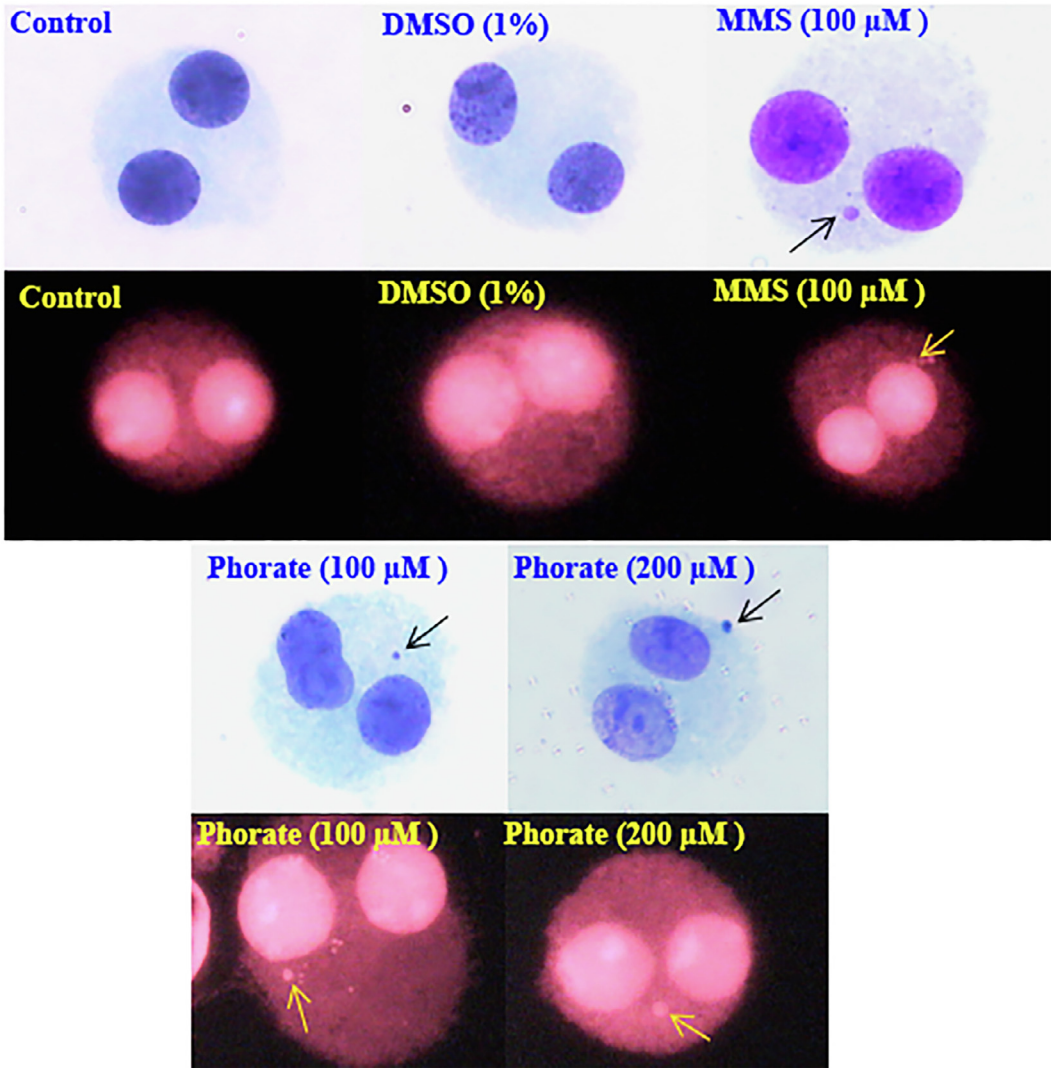

Fig. 2. Representative photomicrographs of the typical binucleated cells showing micronuclei in phorate treated lymphocytes after 24 h of exposure. Cells appearing light blue were stained with 6% Giemsa stain and light pink are the fluorescence of propiodium iodide (6 µg/ml) stained cells belong to the same set of treatments. Arrow indicate the presence of micronuclei in phorate and positive control (MMS) treated cells.

Table 2
Effect of phorate on micronuclei formation in human lymphocytes.

Compound	Dose	BNMN/1000 cells	NDI
Control	0	4.1 ± 1.71	1.94
DMSO Control	1.2%	5.0 ± 1.58	1.95
MMS (µM)	100	15.3 ± 2.97*	1.82
Phorate (µM)	50	11.0 ± 1.41	192
	100	16.5 ± 3.53*	1.89
	200	26.50 ± 2.12*	1.80

MMS: methyl methane sulphonate (as positive control), DMSO: solvent control.
*$p < 0.05$, analyzed by Tukey test.

condition, ct-DNA (500, 1000, 1500 and 2000 ng) exposed to positive control (methylene blue, 1000 µM) showed 1.2, 1.6, 1.7, 1.6-fold 8-oxodG adduct formation (Supplementary Fig. 2).

3.6. DNA breaks after phorate exposure

Selective elution of broken DNA using hydroxyapatite matrix showed enhancement in the single stranded DNA with simultaneous reduction in duplex DNA upon phorate and phorate-Cu (II) treatment (Supplementary Fig. 3). At the highest DNA nucleotide/phorate molar ratio (1:10) plus 100 µM Cu (II), almost equal number of strand breaks were quantitated as obtained with EMS. Strand breaks (n) determined for phorate alone and phorate-Cu (II) exposed DNA were; 1.0, 1.5, 2.2, 2.8, 4.0 and 1.6, 2.8, 3.7, 4.6, 6.5 at DNA nucleotide/phorate molar ratio of 1:2, 1:4, 1:6, 1:8 and 1:10, respectively. The negative control (untreated ct-DNA) did not show any strand breaks. Treatment with EMS (2 mM) taken as positive control has induced 7.0 breaks/unit of DNA (Supplementary Table 1).

4. Discussion

Previously we studied the adverse effects of phorate in rats and WISH cells, as well as demonstrated the conformational alterations in human serum albumin (Saquib et al., 2011, 2012a, 2012b). Despite the toxicological consequences of phorate, we encountered a single study demonstrating the lymphocytic toxicity of phorate (Timoroğlu et al., 2014). However, a substantial information on the mechanism of genotoxic effects in human cells is still obscure. Herein, we selected human peripheral blood mononuclear cells, as a model to unravel the phorate induced toxicity, manifested in the

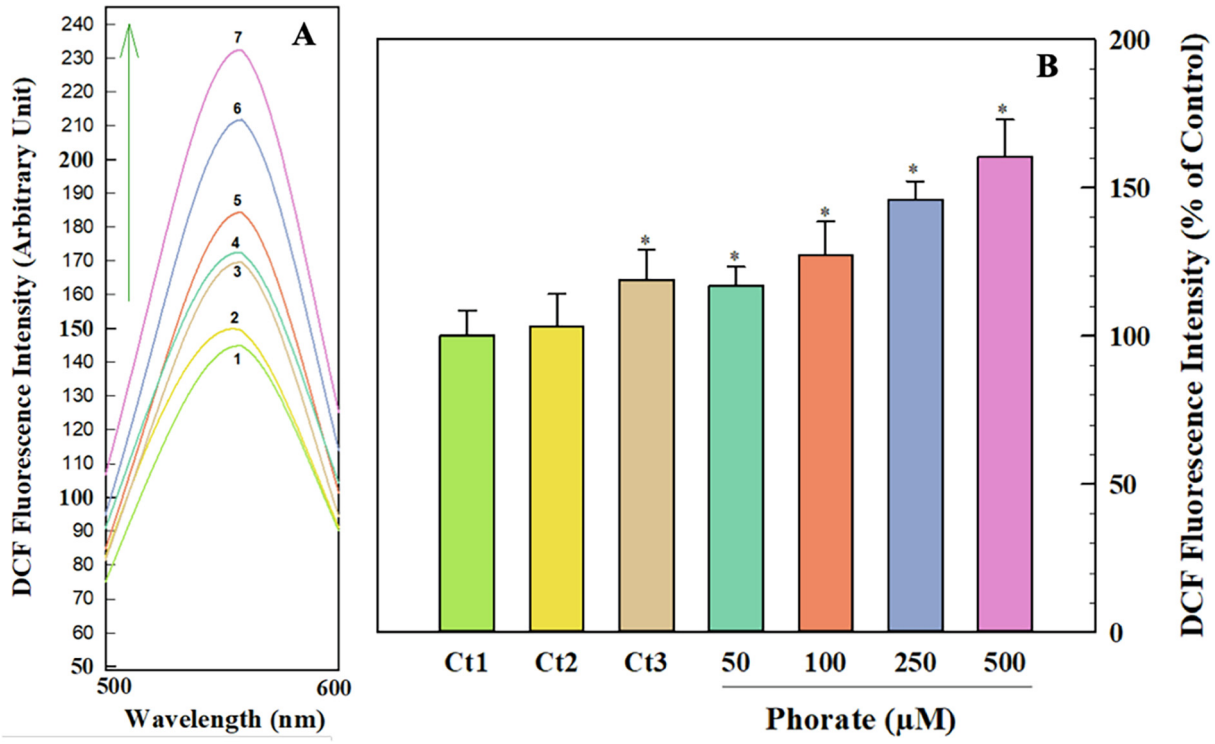

Fig. 3. Intracellular quantitation of ROS by fluorescence spectrophotometer. (A) Emission spectra showing enhanced fluorescence of DCF in lymphocytes treated with varying concentrations of phorate. From bottom to top, spectrum 1: untreated control, spectrum 2: DMSO (1%) solvent control, spectrum 3: phorate 50 μM, spectrum 4: H_2O_2 (400 μM) as positive control, spectra (5, 6 and 7): phorate 100, 250 and 500 μM. (B) The corresponding plot of DCF fluorescence relative to untreated control. Each histogram is the mean ± S.D of three independent experiments. Ct1; untreated control, Ct2; DMSO (1%) solvent control, Ct3; H_2O_2 (400 μM) as positive control. $^*p < 0.05$ vs DMSO control.

terms of cytological changes, DNA fragmentation, dysfunction of $\Delta\Psi m$ and oxidative (8-oxodG) DNA adduct formation. A brief exposure (3 h) of human lymphocytes with varying phorate concentrations increased the damage DNA (Fig. 1). Our comet results are consistent with an earlier finding on phorate induced-DNA damage (Timoroğlu et al., 2014). The CBMN assay revealed significant increase in micronuclei formation in human lymphocytes upon phorate treatment, which corroborates well with the micronuclei formation in phorate treated human lymphocytes (Timoroğlu et al., 2014) and mice (Sobti et al., 1982; Dhingra et al., 1990; Timoroğlu et al., 2014). An increase in the micronuclei formation strongly suggests that phorate triggered DNA damage, which was beyond the error-free repairing capacity of the cellular machinery in cell cycle (González et al., 2003). The appearance of micronuclei in cells are mainly governed by the fragments of acentric chromatid and chromosomes or originate as a consequence of chromosome loss failing which cannot be a part of daughter nuclei and lag behind in cytoplasm during mitosis (Savage, 1988, 2000; Mateuca et al., 2006; Fenech, 2007, 2010; Bonassi et al., 2011). Consequently, micronuclei formation can adversely affect the chromosomal stability in cells. The presence of micronuclei in lymphocytes and its relation with carcinogenesis has been considerably validated in experimental studies (Bonassi et al., 2011). We have observed a significant reduction in NDI of phorate treated lymphocytes. The lower NDI observed after phorate treatment can be extrapolated with following hypothesis that lymphocytes suffers DNA damage (as evident in comet assay), cannot survive the cell division cycle and enters into necrosis or apoptosis before the end of first division. Also, there may be a mitotic delay, hampering the rectification of strand-breaks, such situations inhibit cellular gateway to mitosis, and affect the amount of mononuclear, binuclear, trinuclear or tetra-nucleated cells (Ionescu et al., 2011).

The spectrofluorescence data showed significant enhancement of ROS generation in phorate treated lymphocytes, indicating oxidative stress in cells. Oxidative stress has been categorized as one of the prime factor for severe toxicity in humans exposed to OPs insecticides (Ranjbar et al., 2005). Phorate treated cells also exhibited the alteration of $\Delta\Psi m$. A noticeable shift in the fluorescence peaks with phorate treatment, along with significant reduction in Rh123 intensity unequivocally suggests the dysfunction of inner mitochondrial membrane, and ROS production (Ling et al., 2003; Tay et al., 2005). Changes in inner mitochondrial membrane can lead to increase in the permeability of its external membrane, which liberate the mitochondrial-apoptogenic factors in cytoplasm (Kim et al., 2002). In addition, distraction of $\Delta\Psi m$ frequently leads to degradation of nuclear DNA (Marchetti et al., 1996).

Production of ROS upon phorate treatment unequivocally indicate the induction of oxidative stress in the treated cells. Under oxidative stress more than twenty different types of DNA modifications are formed, including oxidation of sugars, bases and strand breaks. 8-oxodG has received considerable attention due to its mutagenic properties, serve as major oxidative maker. 8-oxodG has been known to induce G → T and G:C → C:G base substitution. The data on phorate induced 8-oxodG formation clearly exhibited higher levels of adduct formation. Considering the genotoxic potential of phorate, we further aimed to quantitated number of breaks in phorate treated ct-DNA. Alkaline unwinding data of phorate and phorate + Cu (II) treatment revealed 4 and 6.5 breaks in ct-DNA (per unit). Involvement of Cu (II) ions in intracellular redox reactions and its affinity for DNA have been extensively studied. The intracellular phorate + Cu (II) and the redox cycling of Cu (II) to Cu (I) along the ct-DNA may also triggers the ROS formation, ultimately resulting in DNA and chromosomal damage, as also evident by the comet and micronuclei data.

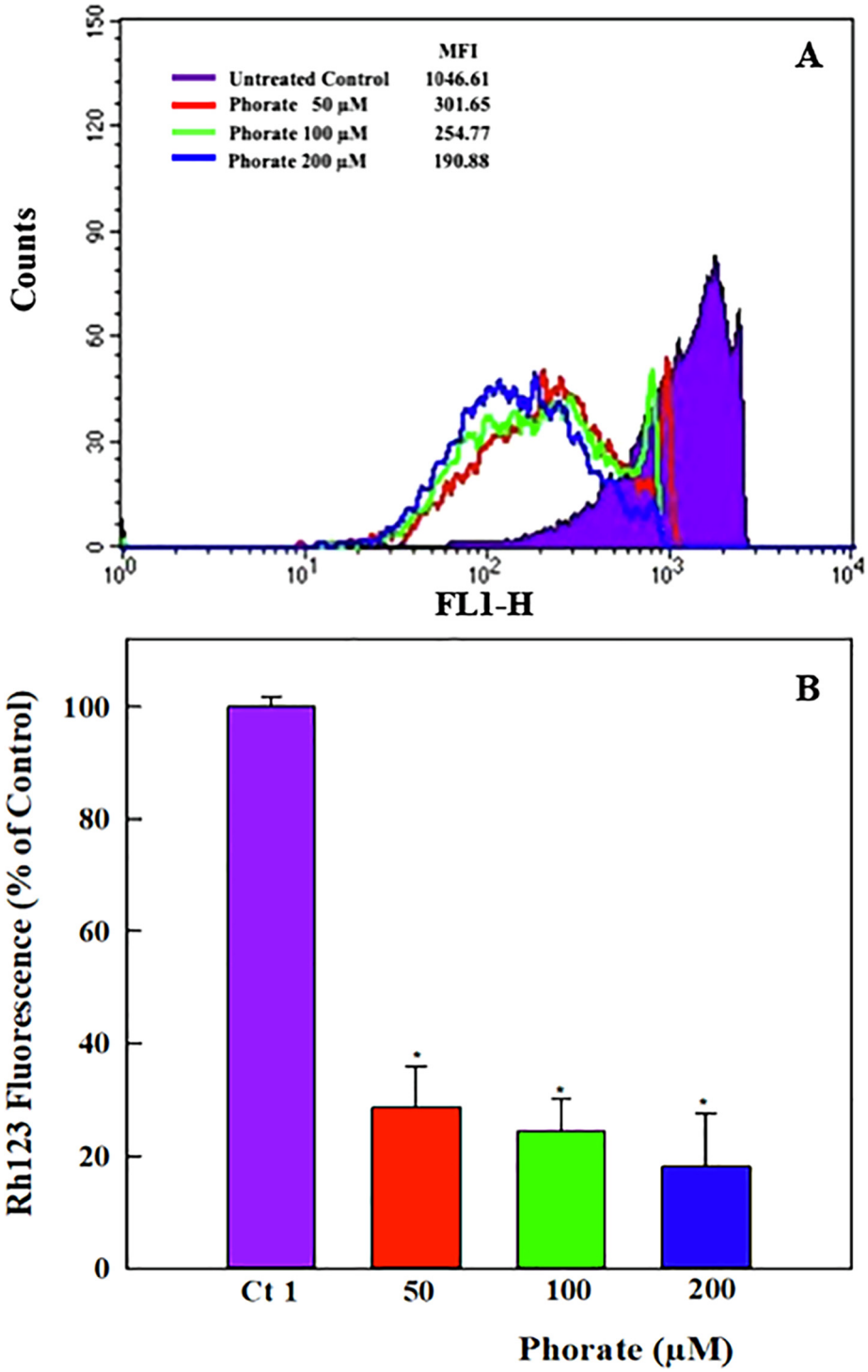

Fig. 4. Phorate induce dysfunction of mitochondrial membrane potential ($\Delta\Psi m$) in human lymphocytes. (A) Representative flow cytometric image showing Rh123 fluorescence in human lymphocytes treated with phorate. MFI: mean fluorescence intensity. (B) Histograms showing Rh123 fluorescence in phorate treated human lymphocytes. Each histogram is the mean ± S.D of Rh123 fluorescence obtained in three independent experiments ($^{*}p < 0.05$ relative to control). Ct 1: untreated control.

5. Conclusion

In conclusion, our data on human lymphocytes exposed to phorate validated its DNA damaging properties in comet assay. CBMN analysis of phorate treated lymphocytes confirm its clastogenic or aneugenic potential, indicating phorate as a cytogenotoxic insecticide. Phorate exposed lymphocytes showed mitochondrial dysfunction. An enhancement in the intracellular ROS unequivocally suggest oxidative stress in phorate treated cells, which preferentially attacks the DNA to increase 8-oxodG adducts and triggers DNA strand breaks. Overall, the data suggest that phorate may also induce similar toxicological consequences in the occupationally or non-occupationally exposed human population. Hence, the application of phorate in various sectors should be given a meticulous attention to avoid human health ailments.

Conflict of interest

The authors declare no conflict of interest.

Acknowledgement

The authors extend their appreciation to the Deanship of Scientific Research at King Saud University for funding this work through research group no (RG-1440-015).

Appendix A. Supplementary data

Supplementary data to this article can be found online at https://doi.org/10.1016/j.sjbs.2019.04.008.

References

Assis, C.R.D., Linhares, A.G., Oliveira, V.M., França, R.C.P., Carvalho, E.V.M.M., Bezerra, R.S., de Carvalho Jr., L.B., 2012. Comparative effect of pesticides on brain acetylcholinesterase in tropical fish. Sci. Total Environ. 441, 141–150.

Bonassi, S., El-Zein, R., Bolognesi, C., Fenech, M., 2011. Micronuclei frequency in peripheral blood lymphocytes and cancer risk: evidence from human studies. Mutagenesis 26, 93–100.

Bonassi, S., Fenech, M., Lando, C., Lin, Y.p., Ceppi, M., Chang, W.P., Holland, N., Kirsch-Volders, M., Zeiger, E., Ban, S., 2001. HUman MicroNucleus project: international database comparison for results with the cytokinesis-block micronucleus assay in human lymphocytes: I. Effect of laboratory protocol, scoring criteria, and host factors on the frequency of micronuclei. Environ. Mol. Mutagen. 37, 31–45.

De Ferrari, M., Artuso, M., Bonassi, S., Bonatti, S., Cavalieri, Z., Pescatore, D., Marchini, E., Pisano, V., Abbondandolo, A., 1991. Cytogenetic biomonitoring of an Italian population exposed to pesticides: chromosome aberration and sister-chromatid exchange analysis in peripheral blood lymphocytes. Mutation Res./Genetic Toxicol. 260, 105–113.

Dhingra, A., Grover, I., Adhikari, N., 1990. Chromosomal aberration and micronuclei assays of some systemic pesticides in bone marrow cells. Nucleus (Calcutta) 33, 14–19.

Dwivedi, S., Saquib, Q., Al-Khedhairy, A.A., Musarrat, J., 2012. Butachlor induced dissipation of mitochondrial membrane potential, oxidative DNA damage and necrosis in human peripheral blood mononuclear cells. Toxicology 302, 77–87.

Fenech, M., 2007. Cytokinesis-block micronucleus cytome assay. Nat. Protoc. 2, 1084.

Fenech, M., 2010. The lymphocyte cytokinesis-block micronucleus cytome assay and its application in radiation biodosimetry. Health Phys. 98, 234–243.

Forsyth, C.S., Chambers, J.E., 1989. Activation and degradation of the phosphorothionate insecticides parathion and EPN by rat brain. Biochem. Pharmacol. 38, 1597–1603.

Garrett, N.E., Stack, H.F., Waters, M.D., 1986. Evaluation of the genetic activity profiles of 65 pesticides. Mutation Res./Rev. Genetic Toxicol. 168, 301–325.

González, M., Soloneski, S., Reigosa, M.A., Larramendy, M.L., 2003. Effect of dithiocarbamate pesticide zineb and its commercial formulation, azzurro: IV. DNA damage and repair kinetics assessed by single cell gel electrophoresis (SCGE) assay on Chinese hamster ovary (CHO) cells. Mutation Res./Genetic Toxicol. Environ. Mutagenesis 534, 145–154.

Grover, I., Malhi, P., 1985. Genotoxic effects of some organophosphorous pesticides I. Induction of micronuclei in bone marrow cells in rat. Mutation Res./Genetic Toxicol. 155, 131–134.

Grover, P., Danadevi, K., Mahboob, M., Rozati, R., Banu, B.S., Rahman, M., 2003. Evaluation of genetic damage in workers employed in pesticide production utilizing the Comet assay. Mutagenesis 18, 201–205.

Ionescu, M.E., Ciocirlan, M., Becheanu, G., Nicolaie, T., Ditescu, C., Teiusanu, A.G., Gologan, S.I., Arbanas, T., Diculescu, M.M., 2011. Nuclear division index may predict neoplastic colorectal lesions. Maedica 6, 173.

Kashanian, S., Askari, S., Ahmadi, F., Omidfar, K., Ghobadi, S., Tarighat, F.A., 2008. In vitro study of DNA interaction with clodinafop-propargyl herbicide. DNA Cell Biol. 27, 581–586.

Kim, R., Tanabe, K., Uchida, Y., Emi, M., Inoue, H., Toge, T., 2002. Current status of the molecular mechanisms of anticancer drug-induced apoptosis. Cancer Chemother. Pharmacol. 50, 343–352.

Lin, M., Wu, C., Wang, T., 1987. Pesticide clastogenicity in Chinese hamster ovary cells. Mutation Res./Genetic Toxicol. 188, 241–250.

Ling, Y.-H., Liebes, L., Zou, Y., Perez-Soler, R., 2003. Reactive oxygen species generation and mitochondrial dysfunction in the apoptotic response to Bortezomib, a novel proteasome inhibitor, in human H460 non-small cell lung cancer cells. J. Biol. Chem. 278, 33714–33723.

Malhi, P., Grover, I., 1987. Genotoxic effects of some organophosphorus pesticides II. In vivo chromosomal aberration bioassay in bone marrow cells in rat. Mutation Res./Genetic Toxicol. 188, 45–51.

Marchetti, P., Susin, S.A., Decaudin, D., Gamen, S., Castedo, M., Hirsch, T., Zamzami, N., Naval, J., Senik, A., Kroemer, G., 1996. Apoptosis-associated derangement of mitochondrial function in cells lacking mitochondrial DNA. Cancer Res. 56, 2033–2038.

Mateuca, R., Lombaert, N., Aka, P., Decordier, I., Kirsch-Volders, M., 2006. Chromosomal changes: induction, detection methods and applicability in human biomonitoring. Biochimie 88, 1515–1531.

Moyer, R.A., McGarry Jr, K.G., Babin, M.C., Platoff Jr, G.E., Jett, D.A., Yeung, D.T., 2018. Kinetic analysis of oxime-assisted reactivation of human, Guinea pig, and rat acetylcholinesterase inhibited by the organophosphorus pesticide metabolite phorate oxon (PHO). Pestic. Biochem. Physiol. 145, 93–99.

Pagliuca, G., Serraino, A., Gazzotti, T., Zironi, E., Borsari, A., Rosmini, R., 2006. Organophosphorus pesticides residues in Italian raw milk. J. Dairy Res. 73, 340–344.

Ranjbar, A., Solhi, H., Mashayekhi, F.J., Susanabdi, A., Rezaie, A., Abdollahi, M., 2005. Oxidative stress in acute human poisoning with organophosphorus insecticides; a case control study. Environ. Toxicol. Pharmacol. 20, 88–91.

Saquib, Q., Al-Khedhairy, A.A., Al-Arifi, S., Dhawan, A., Musarrat, J., 2009. Assessment of methyl thiophanate–Cu (II) induced DNA damage in human lymphocytes. Toxicol. In Vitro 23, 848–854.

Saquib, Q., Al-Khedhairy, A.A., Siddiqui, M.A., Roy, A.S., Dasgupta, S., Musarrat, J., 2011. Preferential binding of insecticide phorate with sub-domain IIA of human serum albumin induces protein damage and its toxicological significance. Food Chem. Toxicol. 49, 1787–1795.

Saquib, Q., Attia, S.M., Siddiqui, M.A., Aboul-Soud, M.A., Al-Khedhairy, A.A., Giesy, J. P., Musarrat, J., 2012a. Phorate-induced oxidative stress, DNA damage and transcriptional activation of p53 and caspase genes in male Wistar rats. Toxicol. Appl. Pharmacol. 259, 54–65.

Saquib, Q., Musarrat, J., Siddiqui, M.A., Dutta, S., Dasgupta, S., Giesy, J.P., Al-Khedhairy, A.A., 2012b. Cytotoxic and necrotic responses in human amniotic epithelial (WISH) cells exposed to organophosphate insecticide phorate. Mutat. Res. 744, 125–134.

Savage, J.R., 1988. A comment on the quantitative relationship between micronuclei and chromosomal aberrations. Mutation Res. Lett. 207, 33–36.

Savage, J.R., 2000. Micronuclei: Pitfalls and problems.

Sobti, R., Krishan, A., Pfaffenberger, C., 1982. Cytokinetic and cytogenetic effects of some agricultural chemicals on human lymphoid cells in vitro: organophosphates. Mutation Res./Genetic Toxicol. 102, 89–102.

Tay, V.K., Wang, A.S., Leow, K.Y., Ong, M.M., Wong, K.P., Boelsterli, U.A., 2005. Mitochondrial permeability transition as a source of superoxide anion induced by the nitroaromatic drug nimesulide in vitro. Free Radic. Biol. Med. 39, 949–959.

Timoroğlu, İ., Yüzbaşıoğlu, D., Ünal, F., Yılmaz, S., Aksoy, H., Çelik, M., 2014. Assessment of the genotoxic effects of organophosphorus insecticides phorate and trichlorfon in human lymphocytes. Environ. Toxicol. 29, 577–587.

Usmani, K.A., Rose, R.L., Hodgson, E., 2003. Inhibition and activation of the human liver microsomal and human cytochrome P450 3A4 metabolism of testosterone by deployment-related chemicals. Drug Metab. Disposition 31, 384–391.

Wauchope, R.D., Buttler, T., Hornsby, A., Augustijn-Beckers, P., Burt, J., 1992. The SCS/ARS/CES pesticide properties database for environmental decision-making. In: Rev. Environ. Contam. Toxicol.. Springer, pp. 1–155.

Williams, F.M., Atherton, K.M., Jamieson, S., Mutch, E., 2006. DNA damage by organophosphate pesticides and repair profiles in human lymphocytes, in vitro. Toxicol. Lett., S261

Zambonin, C.G., Quinto, M., De Vietro, N., Palmisano, F., 2004. Solid-phase microextraction–gas chromatography mass spectrometry: a fast and simple screening method for the assessment of organophosphorus pesticides residues in wine and fruit juices. Food Chem. 86, 269–274.

Zhang, W., 2018. Global pesticide use: profile, trend, cost/benefit and more. Proc. Int. Acad. Ecol. Environ. Sci. 8, 1.